Adhesion measurements in MOS2 dry lubricated contacts to inform predictive tribological numerical models : comparison between laboratory-tested samples and ball bearings from the niriss mechanism

Guillaume Colas, Simo Pajovic, Aurélien Saulot, Mathieu Renouf, Peter Cameron, Alexander Beaton, Andrew Gibson, Tobin Filleter

ADHESION MEASUREMENTS IN MOS_2 DRY LUBRICATED CONTACTS TO INFORM PREDICTIVE TRIBOLOGICAL NUMERICAL MODELS: COMPARISON BETWEEN LABORATORY-TESTED SAMPLES AND BALL BEARINGS FROM THE NIRISS MECHANISM

Guillaume Colas [(1)], Simo Pajovic [(1)], Aurélien Saulot [(2)], Mathieu Renouf [(3)], Peter Cameron [(4)], Alexander Beaton [(4)], Andrew S. Gibson [(5)], Tobin Filleter [(1)]

[(1)] Department of Mechanical and Industrial Engineering, University of Toronto, Canada, E-mail: Guillaume.Colas@utoronto.ca, Simo.Pajovic@mail.utoronto.ca, Filleter@mie.utoronto.ca
[(2)] Université de Lyon, LaMCoS, INSA-Lyon, CNRS UMR 5259, France, E-mail: Aurelien.Saulot@insa-lyon.fr
[(3)] Laboratoire de Mécanique et Génie Civil (LMGC), CNRS, Université de Montpellier, Montpellier, France, E-mail: Mathieu.Renouf@umontpellier.fr
[(4)] Honeywell Aerospace, 303 Terry Fox Dr, Kanata, ON K2K 3J1, Canada, E-mail: Peter.Cameron@Honeywell.com, Alexander.Beaton@Honeywell.com
[(5)] Canadian Space Agency, 6767 route de l'Aéroport, Saint-Hubert, QC J3Y 8Y9, Canada, E-mail: Andrew.Gibson@canada.ca

ABSTRACT

Predicting the tribological behaviour of dry lubricants remains difficult because it greatly depends on their mechanical and physicochemical environment. While it is difficult to analytically model dry lubrication, Discrete Element Method (DEM)-based modelling has been able to provide valuable insight into the tribological behaviour of dry lubricated contacts.

The present study aims to experimentally define interactions between the discrete elements used for simulating different materials in contact, in order to accurately model and predict the tribological behaviour of dry lubricants. Those interactions are here defined by using the work of adhesion (W) between engineering materials: AISI440C, pristine MoS_2 coating, as well as the related transfer film. A method was developed and applied on regular laboratory tribological test samples and ball bearings from the Near Infrared Imager and Slitless Spectrograph (NIRISS) instrument of the James Webb Space Telescope.

Measured W values were consistent between all worn surfaces. The first DEM modelling results exhibit behaviours similar to those observed experimentally including surface plasticization and transfer.

1 INTRODUCTION

Quantitative prediction of the tribological behaviour of a dry lubricant is extremely difficult for several reasons. First, the tribological behaviour depends on multiple parameters from the machine stiffness and degrees of freedom [1], to the microstructure of the tribological materials [2,3], to the physicochemical environment and the reactions it triggers under tribological stresses [3]. Secondly, to quantify the impact of each parameter on the contact behaviour, there is a need to observe within the contact, which is not possible experimentally without disturbing the contact and consequently the measurements. However, it is possible to observe inside the contact numerically and study the influence of parameters such as particle detachment and circulation inside the contact [4].

DEM-based modelling has demonstrated great potential in terms of emulating particle detachment from tribological materials, their circulation and trapping inside the contact, and the formation of a transfer film [5,6]. Studies have already shown good correlation of those models with real applications, for example with composite materials [6]. Recent studies also demonstrated the possibility to model heat transfer [7] and electrical current conduction within the interface [8].

Despite the promising initial studies, those models require multiple inputs in order to efficiently emulate materials. A strong limitation is that it is impossible to directly consider the effect of the changing environments (e.g. humid to dry air, air to vacuum) that in turn impact the cohesion of the transfer film and its adhesion to surfaces, to efficiently lubricate the contacts. To overcome such a limitation, we propose to study those adhesive forces and to develop an experimental approach to reliably and relevantly evaluate adhesion. As adhesion forces are highly dependant on both the materials and geometries in contact (composition, mechanical properties, roughness), we focus on the work of adhesion (W), which is a physical value representative of the contact between two specific materials and independent of the contact geometry.

Herein for the first time, W is determined between stainless AISI440C steel (used in many mechanical components such as ball bearing) and MoS_2 (1 µm thick coating) before and after it underwent friction. The

measurements are done on laboratory samples and on ball bearing from an Engineering Model - Life Test Unit (EM-LTU) of the NIRISS instrument of the James Webb Space Telescope [9]. To ensure reliable comparisons of determined *W* values, morphologies and compositions of the friction/rolling tracks are investigated in detail and compared.

In parallel to the experimental work, the model of the MoS_2 coating is also created to ultimately emulate its tribological behaviour. *W* is to be used as an input to inform the model. The model and related results will be presented.

If laboratory tested samples present similar worn materials characteristics, then it could be possible to avoid long and costly mechanisms testing and use laboratory tests to reasonably inform numerical models which can ultimately help predict mechanisms behaviours.

2 MORPHOLOGICAL STUDIES OF LAB. SAMPLES AND BALL BEARINGS

2.1 Laboratory samples

Laboratory macroscale samples from a previous study [3,10], were subjected to pin-on-plate reciprocating tribometer friction testing in ultrahigh vacuum (UHV) (Figure 1). The maximum Hertz contact pressure was 1 GPa. The full morphological study and tribological life of the material can be found in [10].

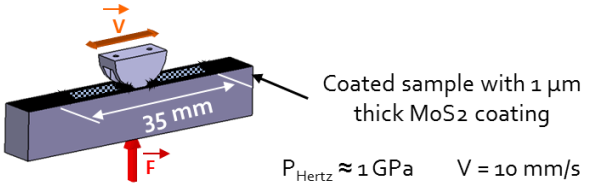

Figure 1 - Tribological tests performed in UHV on the MoS_2 coating. Only the plate sample is coated. Pin and plate samples are made of AISI440C

As shown in Figure 2, lubrication is performed by the 3rd body layer (also called transfer film but less restrictive, details in [11,12]) formed within the contact, separating the pin and the coated plate. Formed due to the agglomeration of the MoS_2 detached particles, the 3rd body layer accommodates velocities by shearing in its volume and plastically flowing inside the contact, and on a second order by sliding on the plasticized top surface (1st body film) of the remaining MoS_2 coating.

Chemical studies have shown that both the 3rd body layer and the 1st body film had the same composition. We should emphasize here that although the friction tests were conducted in UHV (10^{-6} Pa), the MoS_2 underwent strong chemical rearrangement, notable via reaction with internal contaminants to create the MoS_xO_y 3rd and 1st body materials [3,13].

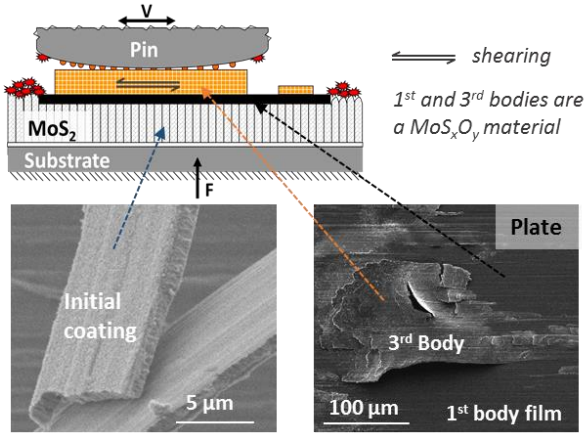

Figure 2 – (Top) Schematics of the contact in laboratory test configuration; (Bottom) SEM images of the coating and the 3rd body trapped in the contact and created during friction.

2.2 Ball bearings

The ball bearings were motor bearings from the EM-life test unit of the Dual Wheel mechanism from the NIRISS instrument [9]. The ball bearing that was lubricated by both PGM-HT (retainer) and MoS_2 coatings (races) underwent a detailed investigation. PGM-HT is a composite material comprised of PTFE, glass fiber, and MoS_2.

The SEM investigation (Figure 3) shows that the MoS_2 coating is heavily damaged, and completely removed in regions of the main rolling track of the races. However, a 3rd body layer remains to ensure lubrication. It is located in the rolling track of the races and on the balls. This layer is very thin (~20 nm) with some thick patches (up to ~300nm) regularly spaced in the rolling track on both the races and the balls. On the ball, the distribution of thick 3rd body "patches" is mainly along one major rolling track (Figure 4), indicating that balls are rolling along one main track, likely with low spinning.

At the ball/retainer contact (Figure 3), there are loose MoS_2 particles trapped in the friction track on the retainer socket. They are believed to (i) act as a reservoir to replenish the contact in case of loss in 3rd body on balls and races; and (ii) accommodate velocities by moving freely inside the contact. Based on their morphology, we can conclude that they come from the MoS_2 particles embedded in the PGM-HT composite retainer.

The elemental chemical analysis done by EDS shows no traces of PTFE, nor glass fibers on the ball and on the

races, not even in the 3rd body. The 3rd body is indeed composed of Mo, S and a low amount of O, which is similar to what was observed on the laboratory samples (Figure 2). That shows that the retainer is minimally worn and only MoS_2 embedded particles are fragmented to form the layer of loose MoS_2 particles at the interface between the ball and the retainer. This is surprising considering that it has been shown that, in the absence of MoS_2 coatings (on both balls and races), the PGM-HT lubricates by transferring MoS_2, PTFE, and glass fiber fragments [14].

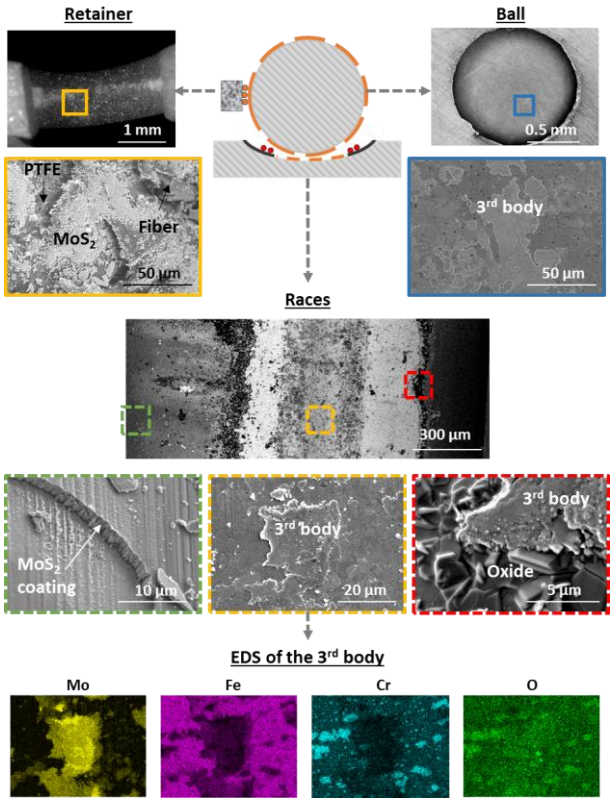

Figure 3 - Ball bearing SEM investigation with EDS chemical analysis of the 3rd body in the rolling track on the race. Color framed SEM images are zoomed in images of low magnification images of each components of the bearing as schematized. EDS analysis of the 3rd body is performed at 10 keV beam energy.

Consequently, the lubrication process appears to involve a double-transfer of lubricant by transferring MoS_2 from the races to the balls and eventually to the retainer. Lubrication is mostly handled by the 3rd body created from the coating initially deposited on the races. PGM-HT has only a small role in the process. Such a behaviour contradicts to some extent what is commonly believed, i.e. that the MoS_2 coating helps lubrication at the beginning, just long enough during the running-in for getting proper lubrication from PGM-HT [15].

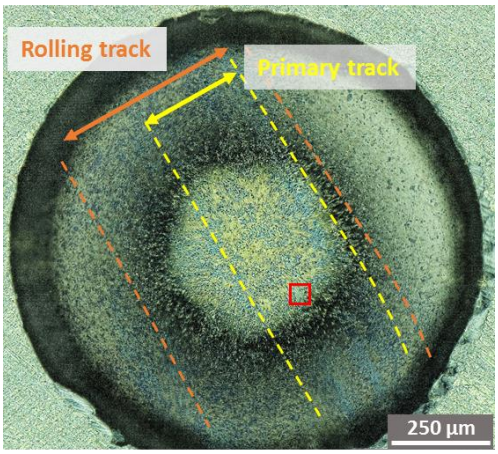

(a)

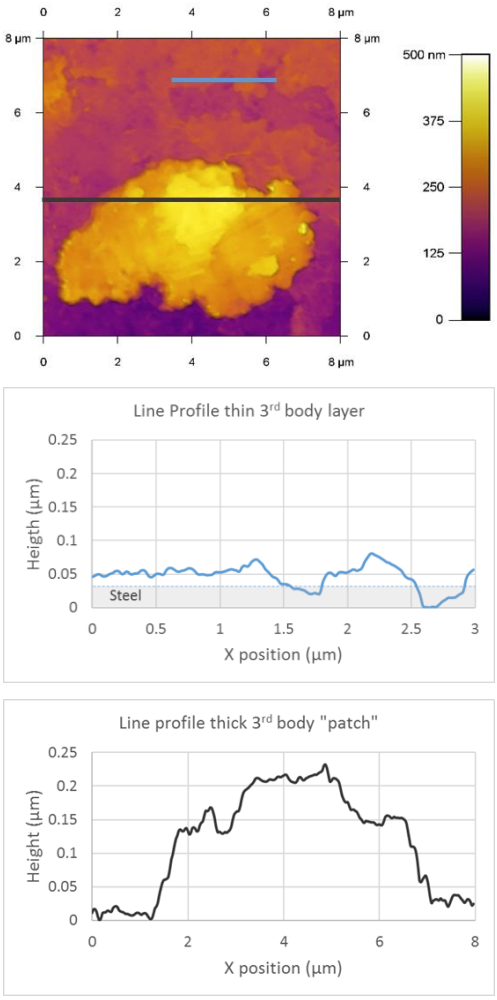

(b)

Figure 4 – (a) Optical image of a ball from the EM-LTU ball bearing, and (b) AFM image and line profiles of the surface showing the thin 3rd body layer and one thick 3rd body "patch"

3 WORK OF ADHESION MEASUREMENTS

As the 3rd bodies observed on both the laboratory samples and on the balls of the ball bearing are similar in terms of morphologies and compositions, *W* can be compared with confidence.

3.1 Method

Using an Atomic Force Microscope (AFM), adhesion forces between AISI440C microbeads, the coating and the 3rd body layer were measured at different stages of the wear life as shown schematically in Figure 5. Measurements were indeed done on laboratory samples at 3 different key stages of the friction life (running in, transient, and steady state) and at humidity of 25% ± 2.5% and 55% ± 5%. On each sample, measurements were done inside and outside (pristine coating) the friction track. The adhesion measurements on the ball bearing are done in 25% ± 2.5% humidity, at steady state, and only on the 3rd body as the coating was not accessible with the AFM. Only results related to the steady states samples (laboratory sample and ball bearing) will be presented. All detailed results as well as the detailed methodology can be found in [16].

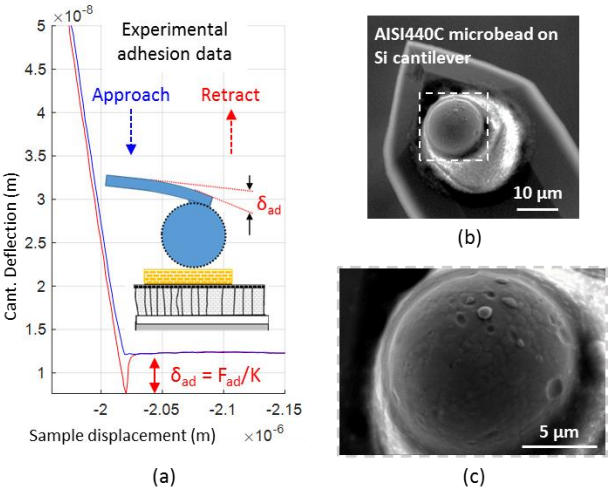

Figure 5 – (a) Adhesion force measurement with AFM. The force of adhesion F_{ad} is measured when the cantilevers is retracted from the surface after elastic contact at a predefined load; K is the cantilever stiffness. (b) and (c) SEM image of the AISI440C microbead glued on AFM cantilevers. (a) and (b) are reproduced from [16]

Once the force measurements were done, a homemade MATLAB script was developed to determine which surface asperities were in contact using experimental data (elastic indentation depth, high resolution images of the microbead and the surface where the contact occurred). Contributions of all asperities in contact during one contact are added. Once the contacting asperities are detected, the Derjaguin approximation is used to determine *W* using equation (1).

$$W = \frac{F_{ad}}{2\pi \sum_{i=1}^{n} R_i^*} \quad (1)$$

where F_{ad} is the measured adhesion force, and R_i^* is the reduced radii of the microbead and the local asperity *i*.

3.2 Results

Figure 6 shows the distribution of measured *W* obtained on the samples of interest for this paper. Regarding the laboratory samples, it can be seen that the distributions of W values are very broad for the pristine coating, from 0.05 to 0.5 J/m^2 with a higher count in the range 0.05 to 0.3 J/m^2. After friction, *W* tends to be primarily in the range of 0.05 to 0.2 J/m^2 with a second minor peak in the range 0.25 to 0.375 J/m^2, followed by a small tail.

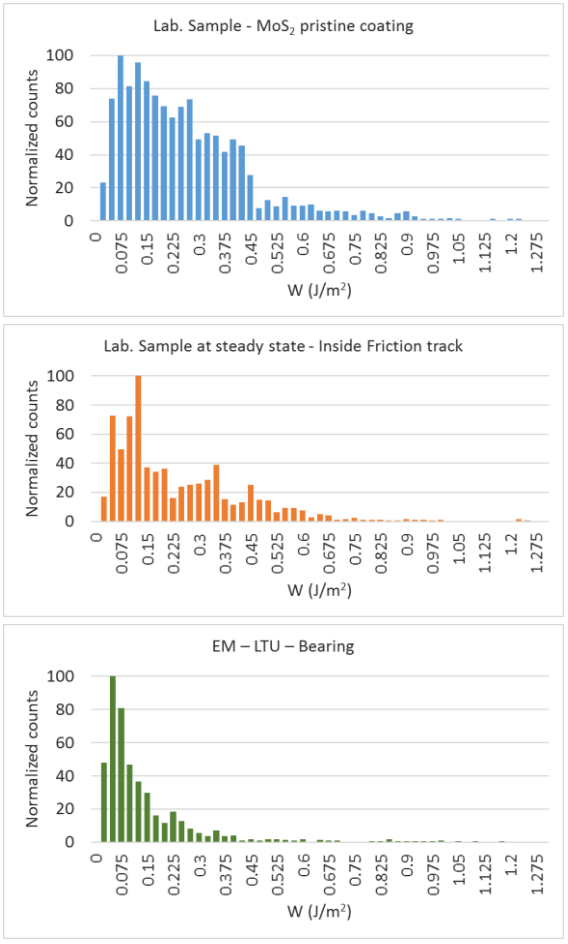

Figure 6 - Work of adhesion (W) between the AISI440C and the pristine MoS_2 coating (all data from the 3 laboratory samples), the MoS_xO_y 3rd and 1st bodies at steady state on the laboratory sample, and the 3rd body from the EM-LTU ball bearing

The change observed in the distributions of *W* values on both the worn and pristine coatings agrees well with the elemental and molecular chemical studies of the samples, and with contact angle measurements. Indeed, the chemistry and contact angles are very different from the inside to the outside. The surface chemistry of the pristine coating is a complex $Mo_xS_yO_z$ while after friction, it becomes a simple MoS_xO_y compounds [13]. This change apparently led to the decrease of the measured contact angle from 74° to 60° after friction [16].

The *W* values measured on the 3rd body created on the ball of the EM-LTU ball bearing (Figure 6) shows similar distributions compared to what was observed on the laboratory samples at steady state. Indeed, the values are mostly in the range 0.05 to 0.15 J/m^2. However, the tail is smaller. This is likely due to the fact that the 3rd body on the ball is more homogeneous and smoother compared to the laboratory sample worn surface. Moreover, there are no signs of bead contamination via transfer of 3rd body particles to the beads. For extremely smooth surface like observed on the 3rd body of the EM-LTU, specific models [16] are required to extract the true *W* which can double the one determined here. Indeed, the only way the data could be processed here was to approximate a very smooth surface as being perfectly flat. Doubling *W* would bring its average value in the same range than what is observed for the laboratory tested sample, inside the friction track. Overall, main *W* values measured on laboratory samples – inside friction track and on the balls are similar, which reflects their similarity regarding their elemental chemical composition.

4 DEM MODELLING

Overall, the consistency of the experimental results suggest that the approach used here provides relevant data for use in numerical simulations that are under development.

4.1 Model description

In order to further understand the mechanism governing the tribological behaviour of MoS_2, a contact between a rigid bead (AFM cantilever) and a MoS_2 coating has been generated in the DEM framework. With such a model it is possible to reproduce an equivalent continuous behaviour [6] but also to account for particle detachment and their evolution within the contact.

The DEM model relies on the 'Non-Smooth Contact Dynamic' framework developed by Moreau and Jean [17,18], and used in several numerical tribological investigations [5-8]. The reader can refer to the original work for more information concerning the method [17,18].

The sample (Figure 7) is based on a real coating (morphology, thickness) in order to model it at 1:1 scale. The numerical sample is composed of 43000 rigid particles reproducing a columnar structure with a given roughness. The roughness of the surface layer is chosen to mimic experimental observation: column diameters range from 210 to 290 nm; the particle diameter is equal to 10 nm ± 2 nm. The height of the sample is equal to 1 µm and its length to 5 µm.

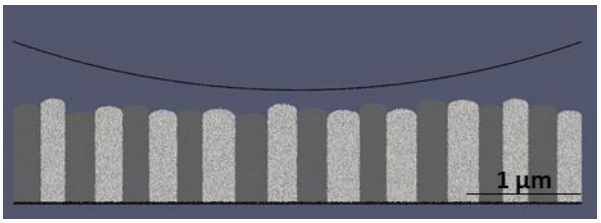

Figure 7 – MoS_2 coating with a columnar structure generated with cohesive discrete elements.

As the geometry is defined, the remaining key point in such modeling concerns the interaction between the different types of discrete elements. As the macroscopic response depends on the local interactions, these last ones should be chosen carefully. The interaction law is characterised by a component in the normal and in the tangential direction (Figure 8). In the normal direction, a unilateral cohesive model is used. It can be seen as a simplification of a Lennard-Jones potential.

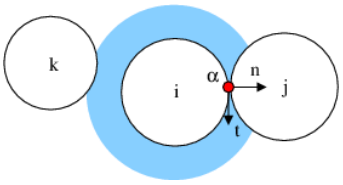

(a)

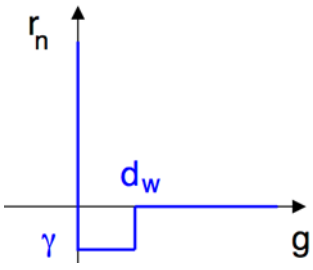

(b)

Figure 8 – (a) Representation of the local contact frame. The blue area corresponds to the attractive zone determine by the d_w value. (b) Illustration of the normal contact law used in the model (g is the distance between elements, r_n is the interaction force between them)

In this sense, the local interaction depends on two parameters: a cohesive force, γ, and an attraction distance, d_w. When a particle enters into the attraction area (blue area of Figure 8), the attractive force acts to minimize the gap between particles. In the tangential direction, a threshold, denoted ν, is given to constrain the motion of the different elements. It can be seen as a local Coulomb friction even if this notion could be confusing at the considered modeling scale.

To respect the columnar structures of the coating, the set of parameters used to control interaction between interacting particles of the same column is different from the set of parameters for interacting particles from two different columns.

The same cohesive force acts between the cantilever and the coating but with a smaller value of γ.

4.2 Indentation Results

As a first approach, indentation tests have been realized on the numerical sample to determine the impact of numerical parameters on the macroscopic response. During such a simulation it is possible to measure the irreversible displacement (Figure 9), which can be associated with plasticization of the coating. In the case of the coating, it can be seen that the deformation is mainly localized at the top of the coating surface, which is something that was observed experimentally on the laboratory samples [10].

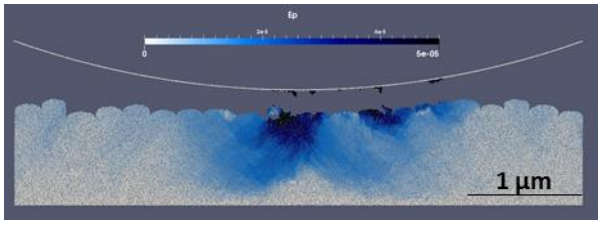

Figure 9 - Visualisation of the irreversible deformation within the MoS_2 coating after an indentation test.

Furthermore, the evolution of the force/displacement curve can be extracted and plotted for different intra column friction values (Figure 10a) and for different column/column cohesion values (Figure 10b).

It can be observed (Figure 10a) that the increase of the internal tangential threshold (ν) increases the force. The higher is the tangential threshold, the smaller is the deformation of the coating. In each case, the adhesive force (negative part of the curve) remains the same and is not affected by this parameter.

When the column/column cohesion force increases, there is no variation on the maximal value of the compressive force neither on the adhesive force (Figure 10b). Indeed, when the cohesion is small, the adhesive force acts on a longer distance.

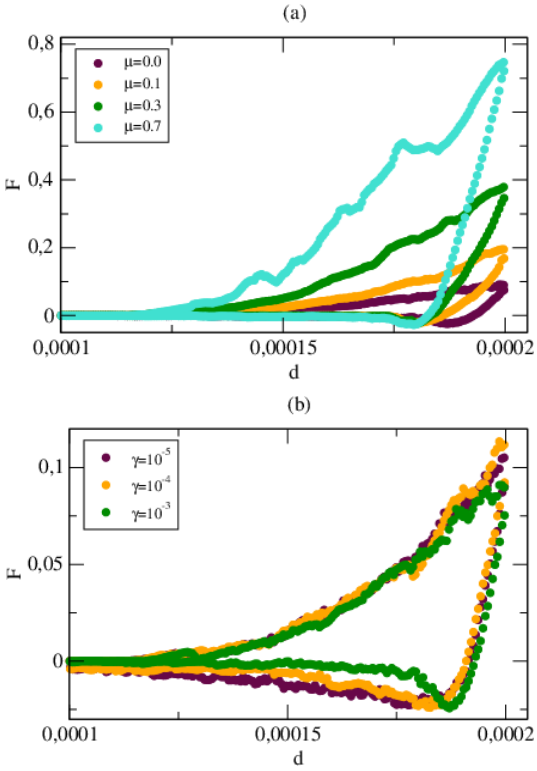

Figure 10 - Influence of (a) the intra-column tangential threshold and (b) the column/column cohesion force on the sample response during an indentation test. The loading force F is in N, the displacement d is in mm.

Moreover, it can be seen on Figure 9 that particles from the coating transfer onto the bead after indentation. Such phenomenon is also observed during the adhesion test measurements. As shown on Figure 11, particles can be transferred to the bead. Even if adhesion measurements are done in the elastic regime of deformation of the coating, locally high pressure can induce very localized plastic deformation and combine with high adhesion to the bead, the particle can become detached and transferred to the surface of the bead. The first DEM indentation modelling, which was intentionally performed in the plastic regime of deformation of the coating, shows such a transfer, and thus correlates well with the experiment.

These results show that via comparison between a numerical parametric study and experimental data, it will be possible to calibrate the different parameter of the models. This would be the case, in a first approach, from a phenomenological point of view. In this first approach, *W* measured experimentally between AISI440C and MoS_2 and between AISI440C and MoS_xO_y 1st and 3rd bodies could be used as ratios, rather than strictly quantitative values.

The first DEM modelling results exhibit behaviours observed experimentally, including the plasticization of the top surface of the coating under compression and the transfer of MoS_2 material to the beads.

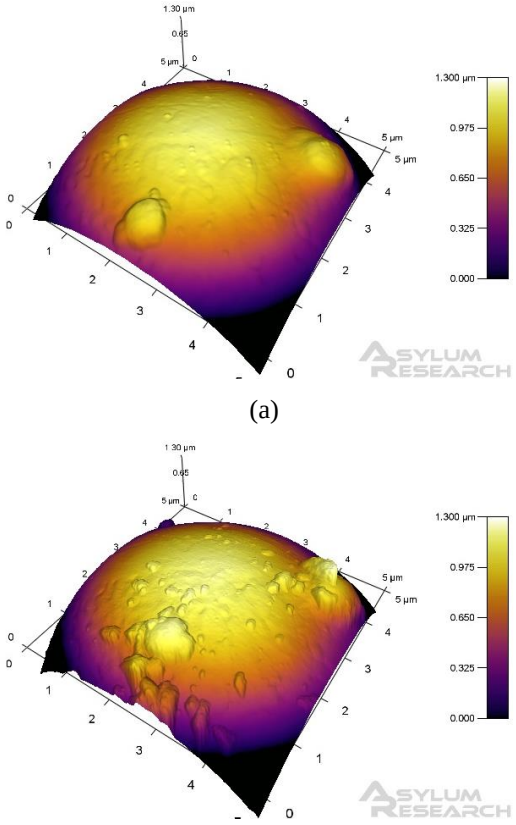

(a)

(b)

Figure 11 - AFM image of on AISI440C microbead before (a) and after (b) adhesion measurements on the pristine MoS_2 coating

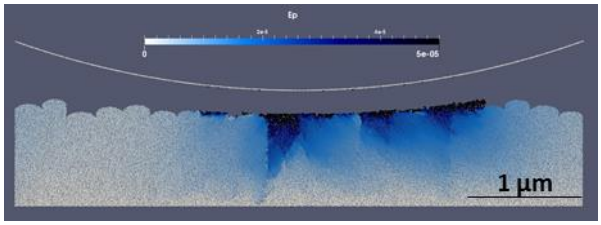

Figure 12 - Loading and reciprocating sliding of the MoS_2 coating.

Complementary to the indentation tests, a prospective result is shown. With such a model, it is possible after the indentation (loading) phase, to impose a sliding motion to the cantilever bead. As shown on Figure 12, the deformed column heads are sheared and flow plastically to form the 1st body film. Experimentally, this occurs and the film eventually detaches from the coating to form a 3rd body after a few sliding cycle. Figure 12 also shows that with the parameter used, for this first test, that deformation propagates vertically along the interface between columns. This will help us to identify the underlying failure mechanisms of the coating.

5 CONCLUSION

The study showed that it is possible to reproduce at the laboratory scale key factors governing the tribological behaviour of dry lubricant (e.g. deformation, particle detachment, transfer, chemical changes) in mechanisms. This study placed particularly emphasis on the 3rd body which was shown to be significantly similar to the one created in mechanism engineering model undergoing life testing. Indeed, the comparisons between the morphology and chemical nature of the contacts in the lab scale and engineering model specimen revealed strong evidence of similarity. Studying the work of adhesion *W* allowed an even stronger direct comparison as it represents the intrinsic interactions between the materials used. Those interactions can be subsequently used as mechanical parameters in DEM modelling under development. The DEM modelling has already shown to effectively reproduce deformation and transfer of materials during normal loading at the contact. Further studies which combine experimental laboratory scale studies with DEM modelling, have great potential to be used in lubricant trade-off studies or to evaluate contact configurations for a specific mechanism. Such a capability could, in particular, reduce the cost of mechanisms development in the long term.

From a ball bearing standpoint, it is worth commenting on the lubrication mechanism in the ball bearing case studied. The morphological studies conducted showed that the lubrication is mainly handled by the MoS_2 coating and not by the PGM-HT. That contradicts some common perceptions. Such a conclusion demonstrates the need for morphological studies of all surfaces coupled with EDS chemical analysis. In the absence of such evidence, it may have been concluded that the PGM-HT was providing effective lubrication for the ball bearing, while instead it was mostly acting as reservoir, even at the end of the life-test.

Finally, while the initial results are promising, substantial additional research is still needed which focuses on the modelling of friction. The DEM model was intentionally created at the scale of the AFM experiment, to allow us to also conduct frictional experiments at the same scale of the model. Hence future direct comparisons will be made between the model and the experiments. Moreover, a complete set of experimental data (quantitative mechanical and friction measurements, morphological analysis of surfaces) will be available to further improve the model accuracy.

6 ACKNOWLEDGEMENT

We would like to thank Ashley McColgan and David Aldridge from Honey Aerospace (Ottawa, Canada) for their support. We would like to thank CDA Intercrop for providing ball bearing parts. We would like to acknowledge support from the Erwin Edward Hart Professorship from the Faculty of Applied Science & Engineering at the University of Toronto. We would also like to thank the Department of Mechanical and Industrial Engineering at the University of Toronto for financial support (Summer research student award, summer 2015), the National Sciences and Engineering Research Council of Canada (Undergraduate Student Research Award, summer 2016, and Engage grant), the French Space Agency for allowing the use of laboratory samples coming from another dedicated study supported by CNES, and the Canadian Foundation for Innovation (CFI) for financial support for equipment used in the work.

7 REFERENCE

[1] Kohen, I., Play, D., Godet, M., (1980), Effect of machine rigidity or degrees of freedom on the load-carrying capacity of wear debris. *Wear*. **61**, 381–384.

[2] Colas, G., Saulot, A., Regis, E., et al., (2015), Investigation of crystalline and amorphous MoS2 based coatings: Towards developing new coatings for space applications. *Wear*. **330**–**331**, 448–460.

[3] Colas, G., Saulot, A., Michel, Y., et al., (2013), Dry Lubrication Efficiency : From Ground To Space. *Conf. Proc. 15th Eur. Sp. Mech. Tribol. Symp.* 25–27.

[4] Renouf, M., Massi, F., Fillot, N., et al., (2011), Numerical tribology of a dry contact. *Tribol. Int.* **44**, 834–844.

[5] Villavicencio, M.D., Renouf, M., Saulot, A., et al., (2016), Self-lubricating composite bearings: effect of fiber length on its tribological proporties by DEM modelling. *Tribol. Int.* In Press.

[6] Champagne, M., Renouf, M., Berthier, Y., (2014), Modeling Wear for Heterogeneous Bi-Phasic Materials Using Discrete Elements Approach. *J. Tribol.* **136**, 21603.

[7] Rivière, J., Renouf, M., Berthier, Y., (2015), Thermo-Mechanical Investigations of a Tribological Interface. *Tribol. Lett.* **58**,.

[8] Zeng, C., Renouf, M., Berthier, Y., et al., (2016), Numerical investigation on the electrical transmission ability of a shearing powder layer. *Granul. Matter*. **18**, 1–7.

[9] Aldridge, D., Gentilhomme, M., Gibson, A., et al., Cryogenic Motor Enhancement for the Niriss Instrument on the, in: Proc. 16th Eur. Sp. Mech. Tribol. Symp. - ESMATS 2015, 2015: pp. 23–25.

[10] Colas, G., Saulot, A., Godeau, C., et al., (2013), Decrypting third body flows to solve dry lubrication issue - MoS2 case study under ultrahigh vacuum. *Wear*. **305**, 192–204.

[11] Godet, M., (1990), Third-Bodies in Tribology. *Wear*. **136**, 29–45.

[12] Berthier, Y., Third-Body Reality - Consequences and use of the Third-Body Concept to Solve Friction and Wear Problems, in: Wear - Mater. Mech. Pract., 2005: pp. 291–317.

[13] Colas, G., Saulot, A., Philippon, D., et al., (2015), Time-of-Flight Secondary Ion Mass Spectroscopy investigation of the chemical rearrangement undergone by MoS2 under tribological conditions. *Thin Solid Films*. **588**, 67–77.

[14] Colas, G., Saulot, A., Descartes, S., et al., (2015), Double Transfer Experiments To Highlight Design Criterion for Future Self-Lubricating Materials. *Conf. Proc. 15th Eur. Sp. Mech. Tribol. Symp.* **2015**, 23–25.

[15] Palladino, M., Report on ESA recommendations regarding PGM-HT use for space applications, 2012.

[16] Pajovic, S., Colas, G., Saulot, A., et al., (2017), Work of adhesion measurements of MoS2 dry lubricated tribological contacts: Comparison between laboratory-tested samples and real mechanisms. *Adv. Eng. Mater.* Submitted.

[17] Moreau, J.J., Unilateral Contact and Dry Friction in Finite Freedom Dynamics, in: J.J. Moreau et al. (Eds.), Nonsmooth Mech. Appl., Springer Vienna, Vienna, 1988: pp. 1–82.

[18] Jean, M., (1999), The non-smooth contact dynamics method. *Comput. Methods Appl. Mech. Eng.* **177**, 235–257.